

Transient Loss Minimization in Induction Machine Drives using Optimal Control Theory

Siby Jose Plathottam, *Member, IEEE*, and Hossein Salehfar, *Senior Member, IEEE*

Abstract-- Loss minimization during transient operation is an often neglected in most induction machine applications. However, loss minimization can greatly improve efficiency in case of fast changing load torques or reference speed profiles. Optimal control theory has been successfully applied previously to develop control laws that minimize losses during transients. All previous works were based on the field oriented induction machine model. In this paper, however, an optimal control problem based on the non-field oriented induction machine model is developed and simulated. Additionally, a more comprehensive cost functional is developed and utilized that would guarantee a stable steady state operation of the machine. Offline optimal control histories are generated using the conjugate gradient method. The performance of the proposed control law is verified through simulation and the results are compared with those from an indirect field oriented controller.

Index Terms— gradient methods, induction motors, optimal control, open loop systems

I. INTRODUCTION

THE ubiquity of induction machines (IM) in industry has led to a large volume of research into improving their efficiency at various operating points. However, it becomes clear from the literature surveys on this topic that a majority of the work has focused on steady state loss minimization [1]. The most common approach to IM loss minimization is to optimize the rotor flux during steady state. But during operating point transitions (change in reference speed or load torque) the loss minimization algorithm is disabled and the flux is maintained at rated level so as to get a faster dynamic performance. This approach is found to be sufficiently adequate since most of the applications involve duty cycles with constant torque-speed operating points. Flux optimization at steady state is already a standard feature in most commercial variable voltage variable frequency (VVVF) drives used in industry. However the utilization of IMs in wind turbines, fly wheel energy storage and electric vehicles (EVs) has opened up a niche of applications where operating point transitions occur in very short time periods. In [2] a study was

conducted where an IM and a permanent magnet synchronous machine (PMSM) used in EVs were compared in terms of energy efficiency for different drive cycles. It was found that the IM operating on a steady state loss minimization could achieve energy efficiencies comparable to that of the permanent magnet synchronous machine.

A literature search by the authors indicated that the amount of literature on transient loss minimization is sparse compared to the literature available on steady state efficiency improvement. Majority of the previous works in this area have utilized optimal control theory. Reference [3] is the most recent and it presents the problem of minimizing rotor, stator and eddy current losses during torque transients. A current fed field oriented model of the induction motor was used. The novelty of [3] is the fact that the model has been reduced to a single differential equation by using a deterministic torque profile. Hence, it was possible to express the loss function in terms of the rotor direct axis flux. The Euler-Lagrange equation was utilized to minimize the loss function and an analytical solution for optimal rotor flux was developed. The same problem was described earlier in [4], and [5] but optimal control laws were developed for the direct and quadrature currents. However in [5] dynamic programming was used to develop an optimal state feedback law while in [4] Euler-Lagrange equation was used. Pontryagin's minimum principle (PMP) was applied to an induction motor control problem in [6] and [7], the objective being to find a minimum time trajectory between two operating points. In this case, an optimal control law was developed for the phase angle between q- and d-axis currents. PMP was utilized again in [8] and [9] with the difference that optimal control laws were derived for the q- and d-axis currents. In addition, it was illustrated that at the end of the transient period the values of the stator currents would be close to the steady state maximum efficiency point. All the previous methods in above are based on the field oriented (FO) model of the IM which requires an estimate or measurement of the rotor position. An error in the rotor position would invalidate the optimal control law.

The present paper is organized as follows; in Section II, the necessary conditions for optimal control arising out of the Pontryagin's minimum principle are briefly introduced. In section III the non-field oriented and field oriented IM

S. J. Plathottam and H. Salehfar are with the Department of Electrical Engineering, University of North Dakota, Grand Forks, ND 58203, USA (e-mail: siby.plathottam@my.und.edu).

models are discussed while section IV derives the necessary conditions. Sections VI and VII are dedicated to the numerical solutions, simulation results, and discussion.

II. PONTRYAGIN'S MINIMUM PRINCIPLE

The Pontryagin's minimum principle (PMP) is one of the two main approaches to optimal control theory, the other being Dynamic programming. PMP has its roots in Calculus of variations but provides a generalized framework for solving both unconstrained and constrained optimal control problems [10]. An optimal control law transfers a system defined by (1) to the required final state within the time t_0 to t_f and minimizes the cost functional given by (2).

$$\begin{aligned} \frac{dx}{dt} &= f(x, u, t) \\ x(t_0) &= x_0 \end{aligned} \quad (1)$$

$$J = \phi(x^{t_f}) + \int_{t_0}^{t_f} g(x, u, t) dt \quad (2)$$

PMP gives a set of necessary conditions that must be satisfied for a control to be optimal. In the case of an unconstrained control variable the necessary conditions are given by (4) to (6) [11]. Here (3) defines the Hamiltonian function, (4) is the costate equation, (5) is the state equation and (6) is the optimal control equation. Equation (5) is the same as the system dynamics defined by (1). L , x and u are the vector of time dependent costates, states, and control inputs for the problem, respectively.

$$H = g(x, u, t) + f(x, u, t)L \quad (3)$$

$$\frac{dL}{dt} = -\frac{\partial H}{\partial x} \quad (4)$$

$$\frac{dx}{dt} = \frac{\partial H}{\partial L} \quad (5)$$

$$\frac{\partial H}{\partial u} = 0 \quad (6)$$

In the problem described in this paper the initial conditions of the states are known while the final states are free. Hence, we use the transversality condition given by (7) to determine the final values of the costates.

$$L(t_f) = \frac{\partial \phi(t_f)}{\partial x(t_f)} \quad (7)$$

The optimal control history is determined by solving the state and costate equations such that it satisfies both the boundary conditions and the optimal control equation.

III. CURRENT FED IM MODEL

Current fed models are preferred over voltage fed models in IM control problems because the former only needs 3 state variables while the latter needs 5 state variables to describe the IM's dynamics. Furthermore, field oriented (FO) current fed model only requires 2 state variables. Optimal control problems (OCP) can be developed for both current fed and voltage fed models but the latter are much more difficult to solve. The non-field oriented (non-FO) and FO IM models are briefly described in this section. The development of IM models are well covered in the literature and readers can refer to [12] for an exhaustive treatment of the same.

A. Non-FO Current fed IM model

Ordinary differential equations (ODEs) which define the non-FO model of the IM in synchronous reference frame are given by (8), (9), and (10). These equations are referred to as the state equations in the context of the optimal control problem. The initial conditions for the model are assumed to be as those given in (12).

$$\frac{d\psi_{qr}}{dt} = -\frac{1}{\tau_r}(\psi_{qr} - L_m i_{qs}) - \psi_{dr}(\omega_e - p\omega_r) \quad (8)$$

$$\frac{d\psi_{dr}}{dt} = -\frac{1}{\tau_r}(\psi_{dr} - L_m i_{ds}) + \psi_{qr}(\omega_e - p\omega_r) \quad (9)$$

$$\frac{d\omega_r}{dt} = \frac{pk}{J}(\psi_{dr} i_{qs} - \psi_{qr} i_{ds}) - \frac{T_l}{J} \quad (10)$$

$$\psi_{qr}^{t_0} = \psi_{qr}^0, \psi_{dr}^{t_0} = \psi_{dr}^0, \omega_r^{t_0} = \omega_r^0 \quad (12)$$

Ψ_{qr} and Ψ_{dr} are the quadratic and direct axis components of the rotor flux respectively while ω_r is the rotor speed and collectively they are the state variables. The control inputs i_{qs} and i_{ds} are the quadrature and direct axis currents respectively. p , J , and T_l are the pole pairs, the moment of inertia and load torque respectively. R_r and L_r are the per phase resistance and inductance of the rotor while L_m is mutual inductance. τ_r is commonly known as the rotor time constant.

The stator, rotor and core loss models are given by (13), (14) and (15), respectively [13]. R_s is the per phase resistance of the stator while R_m is the iron loss resistance. The electromagnetic torque developed at final time is given by (16). All the variables with t_f as superscript correspond to their values at terminal time t_f .

$$P_{loss}^{stator} = (i_{ds}^2 + i_{qs}^2) R_s \quad (13)$$

$$P_{loss}^{rotor} = \frac{1}{\tau_r L_r} \left((\psi_{qr} - L_m i_{qs})^2 + (\psi_{dr} - L_m i_{ds})^2 \right) \quad (14)$$

$$P_{loss}^{core} = \frac{k^2 \omega_e^2}{R_m} \left((L_{lr} i_{ds} + \psi_{dr})^2 + (L_{lr} i_{qs} + \psi_{qr})^2 \right) \quad (15)$$

$$T_e^{tf} = pk \left(\psi_{dr}^{tf} i_{qs}^{tf} - \psi_{qr}^{tf} i_{ds}^{tf} \right) \quad (16)$$

B. FO Current fed IM model

The ODE's which define the FO IM model are given by (17) and (18) with the corresponding initial conditions (19).

$$\frac{d\psi_{dr}}{dt} = \frac{1}{\tau_r} (L_m i_{ds} - \psi_{dr}) \quad (17)$$

$$\frac{d\omega_r}{dt} = \frac{pk}{J} \psi_{dr} i_{qs} - \frac{T_L}{J} \quad (18)$$

$$\psi_{dr}^{t_0} = \psi_r^0, \omega_r^{t_0} = \omega_r^0 \quad (19)$$

The rotor and core loss models (20) & (21) as well as the torque equation (22) are modified on account of ψ_{qr} being 0. The stator core loss model is modified from that given in [13] by assuming that slip is very small.

$$P_{loss}^{rotor} = \frac{1}{\tau_r L_r} \left((L_m i_{qs})^2 + (\psi_{dr} - L_m i_{ds})^2 \right) \quad (20)$$

$$P_{loss}^{core} = \frac{p^2 k^2 L_{lr}^2}{R_m} \omega_r^2 i_{qs}^2 + \frac{p^2 L_m^2}{R_m} \omega_r^2 i_{ds}^2 \quad (21)$$

$$T_e^{tf} = pk \psi_{dr}^{tf} i_{qs}^{tf} \quad (22)$$

IV. OPTIMAL CONTROL LAW USING PMP

The main objective of this paper is to compare performance of OC laws based on both non-FO and FO IM models for a common optimal control problem. The problem is henceforth defined as determining the control history that transfers an IM from an arbitrary set of initial conditions to the specified reference speed and load torque with minimum rotor, stator and iron losses in time t_0 to t_f . The corresponding Bolza form cost functional is given by (23). It must be noted that all the variables inside the integral are functions of time.

$$J = (T_e^{tf} - T_L)^2 + (\omega_r^{tf} - \omega_r^{ref})^2 + \int_{t_0}^{t_f} P_{loss}^{stator} + P_{loss}^{rotor} + P_{loss}^{eddy} dt \quad (23)$$

A. OC with non-FO IM model

The optimal control law is implemented in a cascade configuration with d-q axis current controllers as illustrated in the block diagram shown in Fig.1. The optimal control law functions as a master loop providing set points to the slave loop which can either be a PI or hysteresis controller.

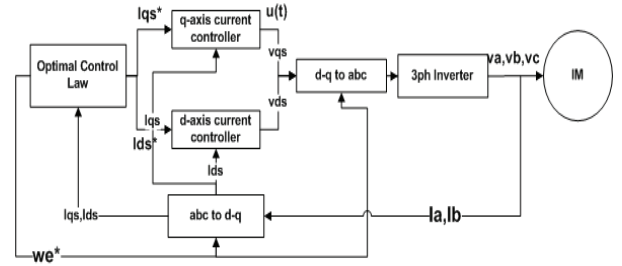


Fig. 1. non-FO Optimal control

The d-q reference frame velocity is also generated by the optimal control law and hence no measurement or estimate of the rotor speed is required. The necessary conditions (4), (5) and (6) are applied to obtain (24) to (30).

$$\begin{aligned} \frac{dL_1}{dt} &= 2(R_r k - k_2 \omega_e^2) i_{qs} - 2 \left(\omega_e^2 k_3 + \frac{1}{\tau_r} \right) \psi_{qr} \\ &+ \frac{1}{\tau_r} L_1 - (\omega_e - p\omega_r) L_2 + \frac{pk}{J} i_{ds} L_3 \end{aligned} \quad (24)$$

$$\begin{aligned} \frac{dL_2}{dt} &= 2(R_r k - k_2 \omega_e^2) i_{ds} - 2 \left(\omega_e^2 k_3 + \frac{1}{\tau_r} \right) \psi_{dr} \\ &+ (\omega_e - p\omega_r) L_1 + \frac{1}{\tau_r} L_2 - \frac{pk}{J} i_{qs} L_3 \end{aligned} \quad (25)$$

$$\frac{dL_3}{dt} = p(\psi_{qr} L_2 - \psi_{dr} L_1) \quad (26)$$

$$\begin{aligned} \frac{\partial H}{\partial i_{qs}} &= 2 \left(k_1 \omega_e^2 + \frac{L_m}{\tau_r} \right) i_{qs} + 2 \left(k_2 \omega_e^2 - \frac{1}{\tau_r} \right) \psi_{qr} \\ &+ 2i_{qs} R_s + \frac{1}{\tau_r} L_1 + \frac{pk}{J} \psi_{dr} L_3 = 0 \end{aligned} \quad (27)$$

$$\begin{aligned} \frac{\partial H}{\partial i_{ds}} &= 2 \left(k_1 \omega_e^2 + \frac{L_m}{\tau_r} \right) i_{ds} + 2 \left(k_2 \omega_e^2 - \frac{1}{\tau_r} \right) \psi_{dr} \\ &+ 2i_{ds} R_s + \frac{1}{\tau_r} L_2 - \frac{pk}{J} \psi_{qr} L_3 = 0 \end{aligned} \quad (28)$$

$$\begin{aligned} \frac{\partial H}{\partial \omega_s} &= 2\omega_e k_3 \left((L_{lr} i_{qs} + \psi_{qr})^2 + (L_{lr} i_{ds} + \psi_{dr})^2 \right) \\ &- L_1 \psi_{dr} + L_2 \psi_{qr} = 0 \end{aligned} \quad (29)$$

$$k_1 = \frac{k^2 L_{lr}^2}{R_m}, k_2 = \frac{k^2 L_{lr}}{R_m}, k_3 = \frac{k^2}{R_m} \quad (30)$$

The final values of the costates are calculated using the transversality condition (7) and given by (31) to (33).

$$L_1(t_f) = 2p^2 k^2 (\psi_{qr} i_{ds}^2 - \psi_{dr} i_{qs} i_{ds}) + 2pk T_L i_{ds} \quad (31)$$

$$L_2(t_f) = 2p^2 k^2 (\psi_{dr} i_{qs}^2 - \psi_{qr} i_{ds} i_{qs}) - 2pk T_L i_{qs} \quad (32)$$

$$L_3(t_f) = 2(\omega_r - \omega_{ref}) \quad (33)$$

B. OC with FO IM model

The concept of using an OC law with FO IM model is illustrated in the block diagram shown in Fig.2. The d-q axis currents are generated by the OC law while the d-q reference frame velocity is calculated as in a standard FOC.

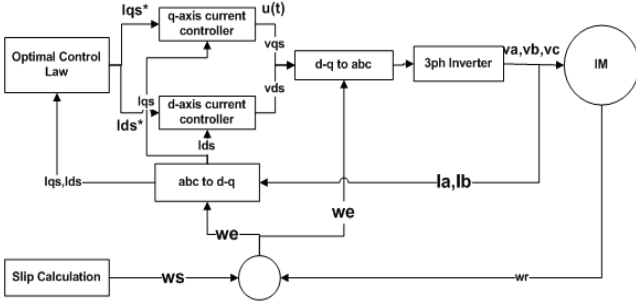


Fig. 2. FO Optimal control

Again we apply the necessary conditions to obtain (34) to (37) and the transversality condition to obtain (38) and (39).

$$\frac{dL_1}{dt} = \frac{2}{\tau_r} (L_m i_{ds} - \psi_{dr}) + \frac{1}{\tau_r} L_1 - \frac{pk}{J} i_{qs} L_2 \quad (34)$$

$$\frac{dL_2}{dt} = -\frac{2p^2}{R_m} (L_r^2 k^2 \omega_r^2 i_{qs}^2 + L_m^2 \omega_r i_{ds}^2) \quad (35)$$

$$\frac{\partial H}{\partial i_{qs}} = 2 \left(\frac{p^2 k^2 L_r^2}{R_m} \omega_r^2 + k^2 R_r + R_s \right) i_{qs} + \frac{pk}{J} \psi_{dr} L_2 = 0 \quad (36)$$

$$\frac{\partial H}{\partial i_{ds}} = 2 \left(\frac{p^2 L_m^2}{R_m} \omega_r^2 + k^2 R_r + R_s \right) i_{ds} - \frac{2kR_r}{L_r} \psi_{dr} + \frac{L_m}{\tau_r} L_1 = 0 \quad (37)$$

$$L_1(t_f) = 2p^2 k^2 \psi_{dr} i_{qs}^2 - 2pk T_L i_{qs} \quad (38)$$

$$L_2(t_f) = 2(\omega_r^{df} - \omega_r^{ref}) \quad (39)$$

V. NUMERICAL SOLUTION

Obtaining an analytical solution for the set of ODE's that comprise the necessary conditions is difficult and hence in this paper a numerical solution is obtained using the gradient method. In this method the state equations are integrated forward and the costate equations are integrated backward from the boundary conditions using a guess control history. Thus the necessary conditions (4) and (5) along with their boundary conditions are automatically satisfied. However the guess control history will not satisfy the optimal control equation (6) in most cases and thus not be the optimal control required. The initial guess control history is improved by updating it in a direction using some algorithm which utilizes the gradient of the Hamiltonian [11]. In this work we utilize the conjugate gradient (CG) algorithm to update the control history as given by (40) and (41). CG method was first proposed in [14] and shown to efficiently solve even non-linear and constrained optimal control problem. The procedure is iterated till the gradient

norm given by (42) reaches an acceptably low value.

$$u^{i+1} = u^i + \tau d^i \quad (40)$$

$$d^i = \begin{cases} -\frac{\partial H}{\partial u}^i, & i=1 \\ -\frac{\partial H}{\partial u}^i + \beta^{i-1} d^{i-1}, & i \geq 2 \end{cases} \quad (41)$$

$$\left\| \frac{\partial H}{\partial u}^i \right\|^2 = \int_{t_0}^{t_f} \left(\frac{\partial H^i}{\partial u^i} \right)^T \frac{\partial H^i}{\partial u^i} dt \quad (42)$$

Since the step length τ in (40) is not optimal, the coefficient β is calculated using the Hestenes-Steifel formula as suggested in [15] is used to calculate the conjugate directions. It must be noted that the processing time required by present day numerical techniques makes them impractical for use with presently available controllers. However since the objective of this paper is to present and compare optimal control concepts and not to develop a practical control system as such, the control history is generated offline for the simulation.

The value of the gradient norm versus the iterations in case of the FO OCP is plotted and shown in Fig. 3. Similar behavior was obtained for the non-FO OCP though the final value of the final gradient norm obtained was an order of magnitude higher compared to the FO OCP. Each torque speed transition corresponds to a separate optimal control problem and there are 100 iterations in each problem.

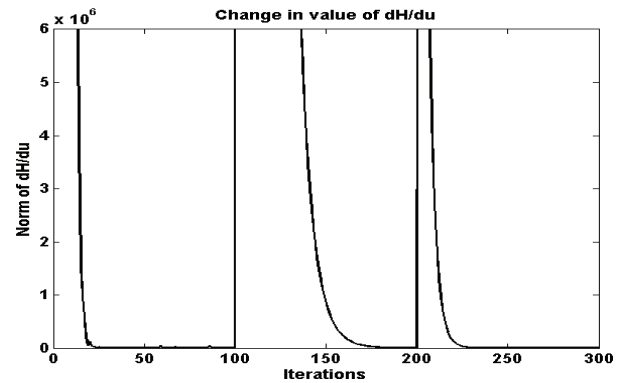


Fig. 3. Change in value of the gradient norm

VI. RESULTS AND ANALYSIS

The authors utilize the voltage fed IM model provided in [12] to compare the performance of the non-FO and FO optimal control laws with that of an indirect field oriented controller (IFOC). A voltage fed model would provide a more rigorous test bed compared to using a current fed model in the simulation. All simulations are performed in Simulink. The per-phase motor parameters are provided in the Appendix of this paper. Initially the IM is generating

zero torque and speed but rotor direct flux has been developed to rated value.

Three load torque and reference speed transitions at 1st, 2nd and 3rd seconds are simulated. The optimal control problems are designed such that the IM should reach steady state 0.5 second after the torque-speed transition.

A. Comparing Torque and Speed

In the first transition, the IM is subjected to its rated load torque of 12.65 Nm and a reference speed of 185 rad/s. In the second transition, load torque and reference speed are half of the previous values. In the final transition, load torque remains the same while reference speed is double of the previous value. Fig. 4 shows the electromagnetic torque generated by the IM while Fig. 5 shows the rotor speed under the three controllers.

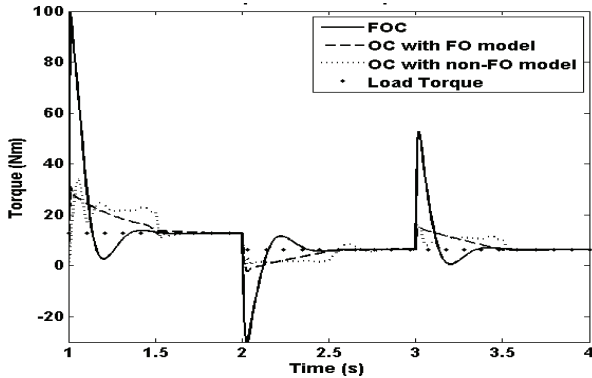


Fig. 4. Comparing electromagnetic torque profiles

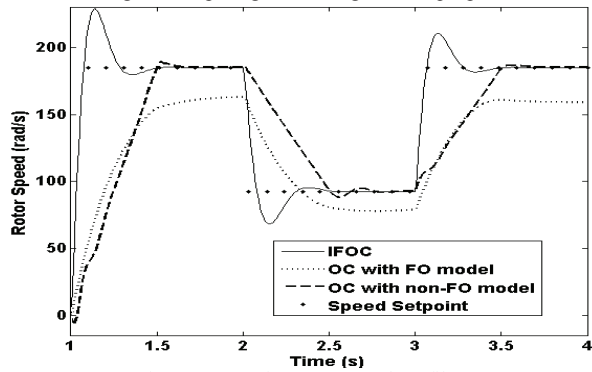


Fig. 5. Comparing rotor speed profiles

It can be observed that the IFOC action causes sharp spikes in the electromagnetic torque at the transition points and enables the motor to settle at its reference speed quickly with no bias error. However, the overshoot causes loss of energy. The optimal control laws (in both cases) have much more subdued torque spikes, almost no overshoot at the transition points, and only take a fraction of seconds more than the IFOC to settle down. Compared to the IFOC, there is a speed bias error present which, though negligible in case of the non-FO optimal control law, is about 20 rad/s for the FO optimal control law and thus significant.

Fig. 6 compares the torque obtained from the solution of

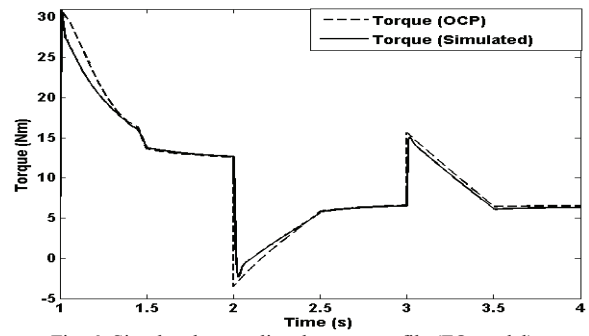


Fig. 6. Simulated vs predicted torque profile (FO model)

the FO optimal control problem compared to the actual torque generated during simulation. The actual torque does not follow the optimal torque because that the IM model used in the optimal control problem is a current fed model and hence does not take into account the stator flux dynamics or the PI current controller dynamics. However at steady state both the torques becomes equal.

B. Comparing Power and Energy Losses

The performance of the controllers in terms of power losses in stator and rotor as shown in Figs. 7 and 8.

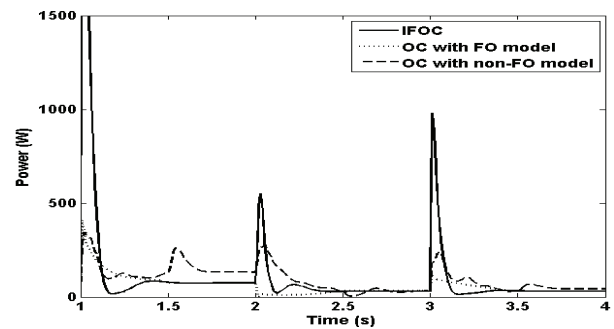


Fig. 7. Stator power loss comparison

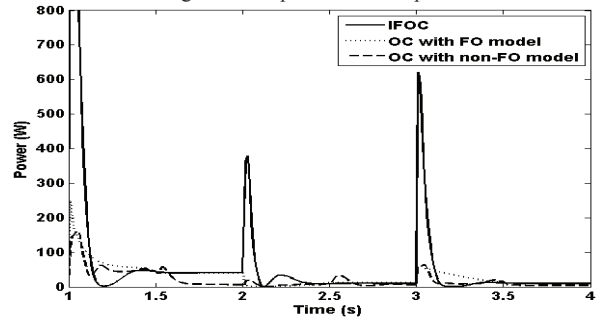


Fig. 8. Rotor power loss comparison

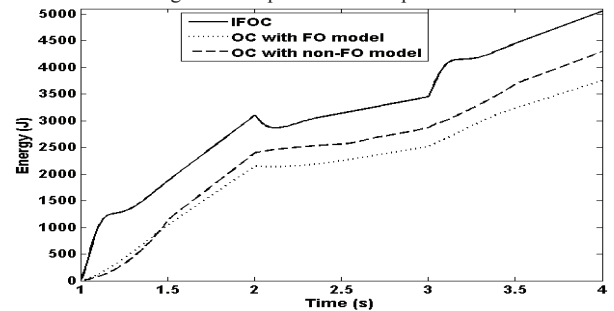


Fig. 9. Stator energy loss comparison

It can be observed that in case of IFOC the torque spikes at the transition points cause power losses which are 3-4 times larger than those due to OC. As was suggested in [2] the cumulative energy consumption for the drive cycle is plotted in Fig. 9 to better appreciate the improvement that is achieved due to the optimal control.

It is evident that non-FO optimal control law reduces energy consumption during the transient period by about 500 Joules on average, compared to that of IFOC for similar steady state torque-speed outputs. In case of the first transition, this is equivalent to a 20% reduction in energy consumption over that from the IFOC. The energy consumption is even lesser in the case of the FO optimal control law. However, this has to be considered in the context of the speed bias error. The energy efficiency for the three cases for the entire 3 second drive cycle is given in Table I.

TABLE I
Drive Cycle Energy Efficiency

Parameter	FOC	FO OC law	Non-FO OC law
Electrical Energy input (J)	5050	3753	4298
Mechanical Energy output (J)	4080	3169	3517
Stator Energy Loss (J)	338	177	288
Rotor Energy Loss (J)	203	89	59
Ohmic energy loss per unit of mechanical energy output	0.13	0.08	0.10
Energy Efficiency (%)	80.8	84.4	81.8

C. Observations

A number of important observations from the simulation results are summarized below.

a) An open loop optimal control law can be stable even if all IM and inner loop dynamics are not considered. However, a low gain trimming feedback loop that engages at the end of the transient period can eliminate the bias error.

b) Transient energy loss minimization is possible during torque-speed transitions without unduly sacrificing performance.

D. Feasibility of an open loop control law

The authors acknowledge that real time implementation of the open loop control law in the form proposed in this paper is difficult. However as stated earlier, that was not the motivation of the authors. Instead it was our stance on the ultimate aim of controller design which we believe should be aimed at preventing errors rather than mitigating errors during disturbances. The IM optimal control problem is inherently capable of providing a solution that satisfies our goal provided the disturbances (load torque and speed setpoint) are known. The OCP can be reformulated as feed forward control law if a closed form solution of the problem is available as has been demonstrated in [3] However these were based on simplifying assumptions of the original optimal control problem. In this paper however the authors chose to represent an IM optimal control

problem in its primal form without being constrained by the necessity of a closed loop solution. The numerical solution generated by the problem for various disturbances will form the basis of designing a feed forward controller.

VII. CONCLUSION

Optimal control theory was applied to both non-FO and FO models of an IM to determine the necessary conditions for a control history that would minimize transient power losses and have an acceptable dynamic performance. Conjugate gradient method was used to obtain numerical solutions of the control law that satisfy the necessary conditions. Simulation results were presented that compared the performance of OC with that of IFOC. It was shown that a significant reduction of energy losses was possible during the transient period without undue sacrifice of the dynamic performance. Furthermore, it was show that OC based on non-FO models can give equivalent results compared to the existing OC approaches that exclusively use FO models. The work in this paper can be further extended by performing hardware experiments.

VIII. APPENDIX

IM D-Q MODEL PARAMETRES

Power: 2.4 kW, Stator resistance R_s : 1.77 Ω , Rotor resistance R_r : 1.34 Ω , Stator inductance L_s :382.8 mH, Rotor inductance L_r :381 mH, Mutual inductance L_m :368.8 mH, Moment of inertia J :0.025 kg-m², Pole pair p :2

IX. REFERENCES

- [1] A. M. Bazzi and P. T. Krein, "Review of Methods for Real-Time Loss Minimization in Induction Machines," *IEEE Trans. Ind. Appl.*, vol. 46, no. 6, pp. 2319–2328, Nov. 2010.
- [2] V. T. Buyukdegirmenci, A. M. Bazzi, and P. T. Krein, "Evaluation of Induction and Permanent-Magnet Synchronous Machines Using Drive-Cycle Energy and Loss Minimization in Traction Applications," *IEEE Trans. Ind. Appl.*, vol. 50, no. 1, pp. 395–403, Jan. 2014.
- [3] J.-F. Stumper, A. Dotlinger, and R. Kennel, "Loss Minimization of Induction Machines in Dynamic Operation," *IEEE Trans. Energy Convers.*, vol. 28, no. 3, pp. 726–735, Sep. 2013.
- [4] C. C. De Wit and J. Ramirez, "Optimal torque control for current-fed induction motors," *IEEE Trans. Automat. Contr.*, vol. 44, no. 5, pp. 1084–1089, 1999.
- [5] R. D. Lorenz and S.-M. Yang, "AC induction servo sizing for motion control applications via loss minimizing real-time flux control," *IEEE Trans. Ind. Appl.*, vol. 28, no. 3, pp. 589–593, 1992.
- [6] S. Sangwongwanich, M. Ishida, S. Okuma, and K. Iwata, "Manipulation of rotor flux for time-optimal single-step velocity response of field-oriented induction machines," *IEEE Trans. Ind. Appl.*, vol. 24, no. 2, pp. 262–270, 1988.
- [7] S. Sangwongwanich, M. Ishida, S. Okuma, Y. Uchikawa, and K. Iwata, "Realization of time-optimal single-step velocity response control of field-oriented induction machines under the condition of nonsaturation of flux," *IEEE Trans. Ind. Appl.*, vol. 27, no. 5, pp. 947–955, 1991.
- [8] J. Rodriguez Arribas and C. M. Vega Gonzalez, "Optimal vector control of pumping and ventilation induction motor drives," *IEEE Trans. Ind. Electron.*, vol. 49, no. 4, pp. 889–895, Aug. 2002.
- [9] C. M. Vega Gonzalez, J. Rodriguez Arribas, and D. Ramirez Prieto, "Optimal Regulation of Electric Drives With Constant Load

- Torque," *IEEE Trans. Ind. Electron.*, vol. 53, no. 6, pp. 1762–1769, Dec. 2006.
- [10] D. Liberzon, *Calculus of Variations and Optimal Control Theory: A Concise Introduction*. Princeton University Press, 2012.
- [11] D. E. Kirk, *Optimal Control Theory: An Introduction*. Dover Publications, 2004.
- [12] N. Mohan, *Advanced Electric Drives: Analysis, Control and Modeling Using Simulink*. MNPERE, 2001.
- [13] S. Lim and K. Nam, "Loss-minimising control scheme for induction motors," *IEE Proceedings- Electr. Power Appl.*, vol. 151, no. 4, pp. 385–397, 2004.
- [14] L. Lasdon, S. Mitter, and A. Waren, "The conjugate gradient method for optimal control problems," *IEEE Trans. Automat. Contr.*, vol. 12, no. 2, pp. 132–138, Apr. 1967.
- [15] E. K. P. Chong and S. H. Zak, *An Introduction to Optimization*. Wiley, 2011.

X. BIOGRAPHIES

Siby Jose Plathottam (M'2015) received his Bachelor's degree in electrical engineering from Mahatma Gandhi University and his Masters degree in control systems from National Institute of Technology Calicut (India). He is currently pursuing his PhD in Engineering from University of North Dakota. His research interests are in optimal control and renewable energy.

Hossein Salehfar (M'1980, SM'1999) received his Bachelor of Science (B.S.) degree in Electrical Engineering from the University of Texas at Austin, and his Master of Science (M.S.) and Doctorate (Ph.D.) degrees in Electrical Engineering from the Texas A&M University in College Station. He was an Assistant Professor of Electrical Engineering at Clarkson University in New York during 1990-1995. Since 1995 he has been with the Department of Electrical Engineering at University of North Dakota, Grand Forks, where he is now a full Professor and the Director of Engineering Ph.D. Program and Interim Associate Dean of College of Engineering. Dr. Salehfar has worked as a consultant for the New York Power Pool, electric utilities and coal industries in the State of North Dakota, and the North Dakota Energy and Environmental Research Center (EERC). Dr. Salehfar has very active and externally funded multidisciplinary research projects. Some of the projects he has worked on include alternative and renewable energy systems, fuel cell technologies, power electronics, electric drives, neuro-fuzzy intelligent systems, electric power and energy systems, power systems reliability, engineering systems reliability, power systems production costing, energy and load management, and energy efficiency. He has supervised several Ph.D. and Masters level graduate students and has published his research work extensively in various journals, conferences, and books. He is a professional member of the American Society for Engineering Education (ASEE) and a senior member of the IEEE.